Supplementary Information (SI) for RSC Sustainability.
This journal is © The Royal Society of Chemistry 2024

Supporting Information

Using waste to treat waste: Efficient alcoholysis of PET waste with shrimp shell derived catalyst using the response surface method

Ruiyang Wen, Guoliang Shen, Meiqi Zhang, Lejia Yang,*

Linlin Zhao, Haichen Wang, Xingzhu Han

(School of Petrochemical Engineering, Shenyang University of Technology, Liaoyang, 111003, China.)

1. Materials section

1.1 Materials and methods

Waste PET bottles are obtained from mineral water bottles. After the removal of the cap and label, they are cut into PET sheets (size: area 3 × 3 mm) and washed and dried. Sodium hydroxide, ethanol (EtOH), and ethylene glycol (EG) are obtained from Chinese medicine reagents (analytical purity), and deionized water is produced in the laboratory.

Powder XRD was performed on Bruker D8, with text rate at 10 °/min. SEM images and elemental compositions of the catalyst were recorded on FEI NOVA NANO450, and TED PELLAINC. FT-IR spectra was recorded on a Bruker FT-IR, using KBr disks. The samples were pre-treated at a degassing temperature of 150 °C for 6 h. ^{1}H-NMR as performed on Bruker, 400 MHz NEO-400 spectrometer in $CDCl_3$ (TMS as internal standard).

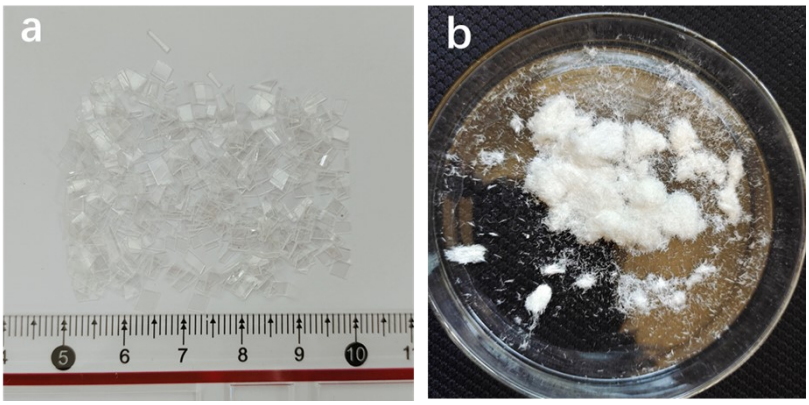

Fig. S1 The size of PET sheet and appearance of the PET and BHET

1.2 Clycolysis of PET waste

1.2.1 Selection of catalysts

The catalytic activity of X-500, X-600 and X-700 was tested to determine their effectiveness. The yield of BHET and the residual rate of L-PET were investigated using a catalyst dosage of 1.00%, 12 ml of EG and a reaction temperature of 195 °C. Fig.S2 (a) shows that the yield of BHET does not consistently increase with depolymerization time, but instead decreases after reaching a dynamic equilibrium of depolymerization-polymerization. Prolonging the reaction time not only increases energy consumption but also does not have a

positive effect on the yield of BHET. The figure show that the X-700 catalyst has the highest catalytic activity, resulting in 81.49% BHET yield and 10.26% L-PET residual rate (Fig .S2(b)) after 3 h of reaction. Subsequently, the research was carried out using X-700 as the catalyst.

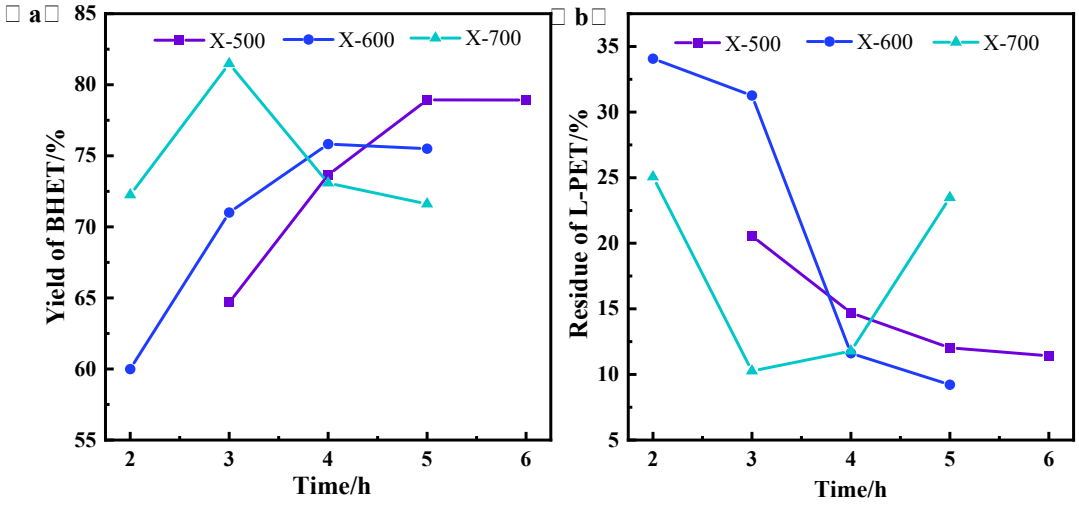

Fig. S2 Screening of the catalytic activity of three catalysts

The correlation function expression is:

$$Y = Yield\ of\ BHET(\%) = \frac{\frac{m_{BHET}}{M_{BHET}}}{\frac{m_{PET0}}{M_{PET}}} \times 100\%$$

$$C = Conversion\ of\ PET(\%) = \frac{m_{PET0} - m_{PET}}{m_{PET0}} \times 100\%$$

where， m_{BHET} is the weight of BHET obtained after degradation, M_{BHET} is the molar weight of BHET (254 g/mol), m_{PET0} is the initial weight of PET, M_{PET} is the molar weight of the repeating unit corresponding to PET (192 g), and m_{PET} is the weight of PET after the reaction.

1.2.2 Responsive surface methodology design

Previously, it was determined that X-700 exhibited superior catalytic activity. However, in order to conduct response surface analysis, it is necessary to establish the range of each influencing factor, including the level range of the coding value. Therefore, we must determine the range of influence of the four factors that significantly impact the PET depolymerization

process through single-factor experiments. We will then identify the two factor values around the relative highest point and the highest point to establish the response surface level, that are: Time，2-4 h; Temperature, 190-200 ℃; Catalyst dosage, 0.50-1.00%; EG volume,10-14 ml.

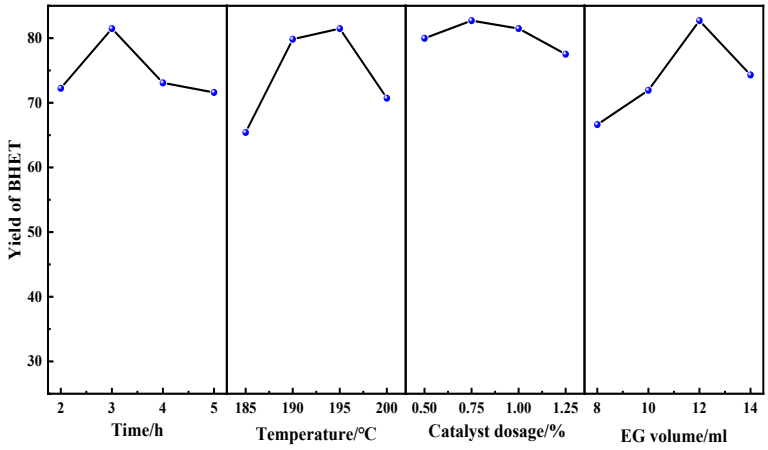

Fig. S3 Determination of the level of single factor

2 Results and discussion

2.1 Characterization and analysis of PET degradation products

The in-plane bending vibration of C-C=O is observed at 656.6-456.6 cm^{-1}, while the vibration peak at 1129.3 cm^{-1} is attributed to the vibration of C-O. When these two vibration peaks are considered in conjunction with the aforementioned observations, it can be concluded that during the depolymerization of PET to L-PET and ultimately to BHET, the vibration peaks of C-C=O and C-O undergo a transition from weak to strong, which aligns with the molecular structure observed between the three compounds. The observed vibration at 3506.0-3266.1 cm^{-1} provides compelling evidence that the -OH group is present in L-PET, which is consistent with the molecular structure of PET and L-PET. However, in BHET, the vibration peak of the hydroxyl group shifts to a lower wave number. This is due to an increase in the concentration of hydroxyl groups, which change from a free state to an intramolecular association. The transformation of the molecular structure was demonstrated by the alteration of the FT-IR functional groups.

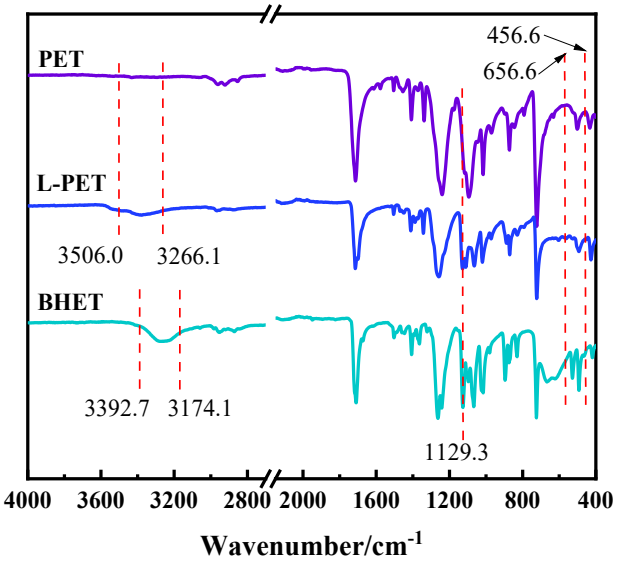

Fig. S4 FT-IR analysis of BHET

Following the FT-IR analysis, the DSC analysis was conducted. The absorption peak of PET exhibited a broad range of 142.9 to 174.1 °C. The presence of oligomers in L-PET led to a broadening of the absorption peak range near 113.5 °C. The absorption peak of oligomers appeared at 188.1 °C. In contrast, BHET only had a narrow absorption peak at 113.5 °C, indicating that there was only one component, which did not contain oligomers, thereby proving the high efficiency of the separation process.

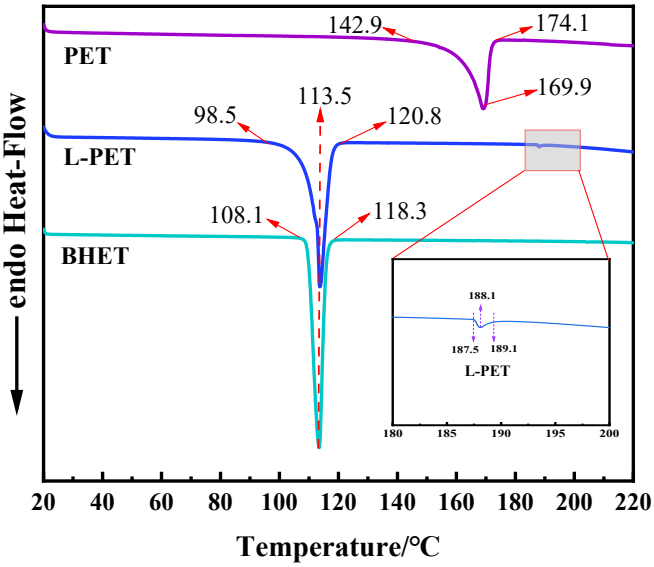

Fig. S5 DSC analysis of degradation product

The ^{1}H-NMR spectrum of the purified product is presented in Fig. S6. The observed chemical shift values are consistent with the proposed structure of H, which corroborates the identity of the isolated product as BHET.

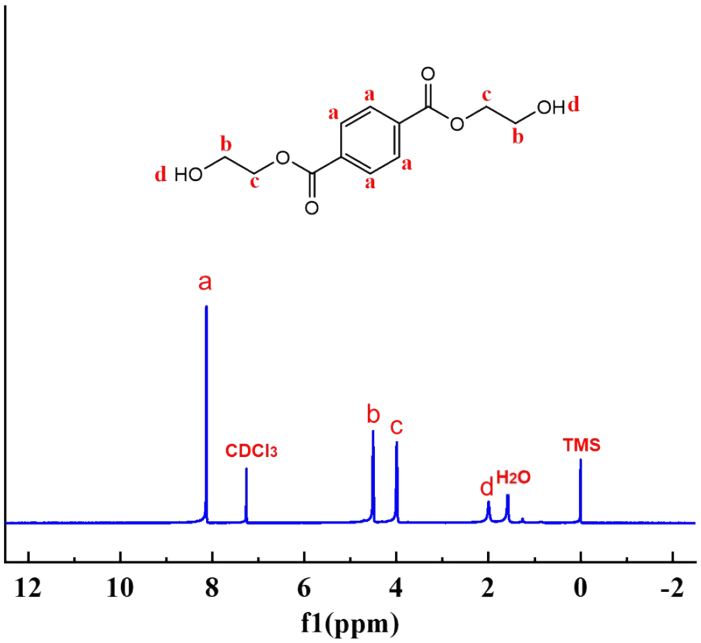

Fig. S6 ^{1}H NMR analysis of BHET

2.2 Optimization of RSM

Based on the preliminary experiments described above, the results of the full factorial BBD design with three levels of four factors and the BHET yields are presented in Tab. S1.

Tab. S1 Results of the experimental and predicted values

Run	A	B	C	D	Yield of BHET/%		Residual/%
					Actual	Predicted	
1	-1	0	0	-1	66.20	67.03	-0.84
2	0	1	0	1	75.58	77.55	-1.97
3	0	0	-1	-1	67.55	68.04	-0.49
4	0	-1	0	-1	69.16	65.84	3.33
5	0	-1	-1	0	73.24	73.65	-0.41
6	1	0	0	-1	68.20	69.72	-1.52
7	-1	0	0	1	77.85	77.05	0.80
8	1	-1	0	0	75.92	76.96	-1.04
9	0	0	0	0	77.65	77.98	-0.33
10	1	1	0	0	75.91	73.36	2.55
11	0	1	1	0	77.60	77.90	-0.31
12	0	0	-1	1	78.60	79.88	-1.27
13	1	0	1	0	76.27	76.51	-0.25
14	1	0	-1	0	76.83	76.69	0.14
15	1	0	0	1	77.42	77.30	0.12
16	-1	-1	0	0	65.79	68.98	-3.19
17	0	0	0	0	78.82	77.98	0.84
18	0	0	0	0	77.92	77.98	-0.06

19	0	0	0	0	79.89	77.98	1.91
20	0	1	-1	0	78.00	77.57	0.43
21	0	0	1	-1	73.05	72.42	0.64
22	0	-1	0	1	80.10	77.63	2.47
23	0	0	0	0	75.63	77.98	-2.35
24	0	0	1	1	78.03	78.18	-0.14
25	-1	1	0	0	78.81	78.41	0.41
26	0	1	0	-1	70.63	71.75	-1.11
27	-1	0	1	0	77.77	76.56	1.21
28	0	-1	1	0	74.84	75.99	-1.15
29	-1	0	-1	0	75.31	73.70	1.60

Statistical analysis of the model was conducted using ANOVA, and the results of the coding variable levels are presented in Tab. S2. The Model F-value of 6.82 implies the model is significant, the order of A, B, C, and D' s F-value is D＞B＞A＞C, the results demonstrate that the impact of EG volume on the model operation process is the most pronounced among the four factors. This indicates that the degradation process of PET is predominantly influenced by alterations in the EG volume parameter. There is only a 0.05% chance that an F-value this large could occur due to noise. The F value of the lack of fit is 2.08, indicating that the lack of fit is not significant relative to the pure error, and the non-significant lack of fit is good, so that the model is more fitted. The signal-to-noise ratio is 9.275, greater than 4, indicating that the signal is sufficient; the standard deviation (Std. Dev = 2.10), mean error (Mean = 75.12), and deviation coefficient (C.V. % = 2.80) of the model indicate that the error is minimal and that the model exhibits a reasonable positive bias within an acceptable error range. The model can be used in experimental design.

Tab. S2 Results of analysis of variance

Source	Sum of squares	Degrees of freedom	Mean Square	F value	P value	Significant [a]
Model	423.25	14	30.23	6.82	0.0005	significant
A	6.49	1	6.49	1.46	0.2463	
B	25.47	1	25.47	5.75	0.0310	
C	5.37	1	5.37	1.21	0.2895	
D	232.18	1	232.18	52.40	0.0000	
AB	42.47	1	42.47	9.58	0.0079	
AC	2.29	1	2.29	0.52	0.4839	
AD	1.48	1	1.48	0.33	0.5721	
BC	1.01	1	1.01	0.23	0.6412	
BD	8.96	1	8.96	2.02	0.1769	
CD	9.24	1	9.24	2.08	0.1708	
A^2	25.53	1	25.53	5.76	0.0308	

B^2	15.98	1	15.98	3.61	0.0784	
C^2	0.11	1	0.11	0.02	0.8767	
D^2	67.29	1	67.29	15.19	0.0016	
Residual	62.03	14	4.43			
Lack of Fit	52.05	10	5.20	2.08	0.2496	not significant
Pure Error	9.99	4	2.50			
Cor Total [b]	485.28	28				

Std. Dev=2.10; Mean=75.12; C.V.%=2.80; R^2=0.8722

The following figure shows the relationship between the response surface prediction and the experimental BHET yield, and the experimental values are fitted and analyzed. The experimental values have a good linear regression, and the whole is close to the regression line, with R^2 of 0.8722 and Adj R^2 of 0.7443.

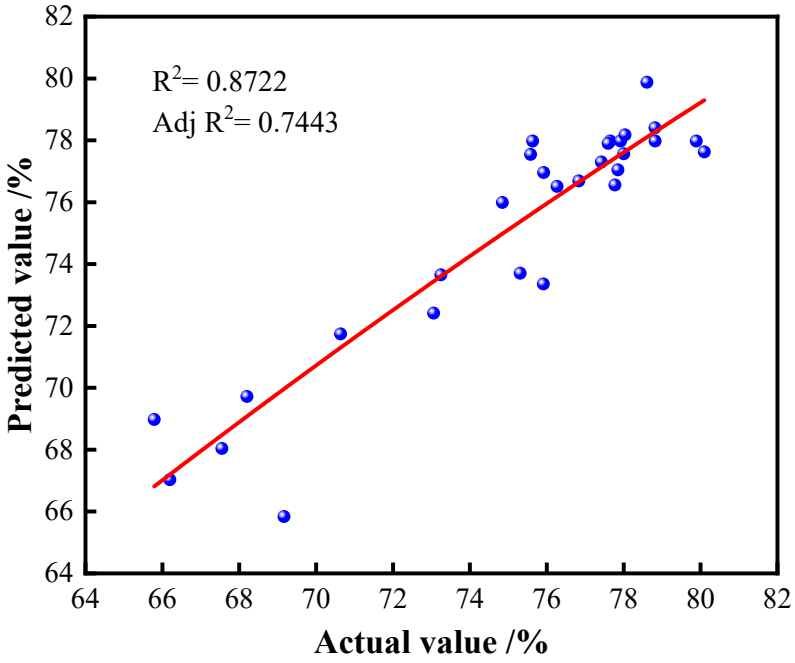

Fig. S7 Comparison of experiment and model results in the BBD

Using the BBD model, the quadratic regression equation of BHET yield can be established：

$$Y = 77.98+0.7353A+1.46B+0.6690C+4.40D-3.26AB-0.7569AC-0.6090AD-0.5013BC-1.50BD-1.52CD-1.98A^2-1.57B^2-0.1307C^2-3.22D^2$$